IranJOC

Iranian Journal of
Organic Chemistry

Experimental kinetics investigation of stable phosphorus ylides involving a theophylline along with theoretical calculations

Majid Moradian[a], Mostafa Habibi-Khorassani*[a], Ali Ebrahimi[a], Malek Taher Maghsoodlou[a], Mohammad Zakarianezhad[b] and Zohreh Khajehali[a]

[a] *Department of Chemistry, University of Sistan and Baluchestan, P. O. Box 98135-674, Zahedan, Iran*
[b] *Department of Chemistry, Faculty of Science, Payam Noor University , Sirjan Center , Sirjan , Iran*

Abstract: In the present work, NMR, theoretical, Kinetics and mechanism investigations were undertaken from a one-pot condensation reaction between theophylline and dialkyl acetylenedicarboxylates in the presence of triphenylphosphine containing novel stable phosphorus ylides **4a-c**. Herein, theoretical calculations have been employed for assignment of the most stable isomers (*Z* or *E*) of phosphorus ylides **4a,b** by natural population analysis, atoms in molecules methods and CHelpG keyword, in which *Z*-**4(a,b)** are more stable forms as the majors. The ^1H, ^{13}C and ^{31}P NMR data of these ylides are consistent with results obtained from theoretical calculations. In addition, kinetic investigation of new ylides was undertaken by ultraviolet spectrophotometry. Useful information was obtained from studies of the effect of solvent, structure of reactants (different alkyl groups within the dialkyl acetylenedicarboxylates) and also the concentration of reactants on the rate of reactions. Proposed mechanism was confirmed according to the obtained results and steady stat approximation and the first and the third (k_3) steps of reaction were recognized as the rate determining and fast steps, respectively on the basis of experimental data.

Keywords: Stable phosphorus ylides; Dialkyl acetylenedicarboxylates; Z and E isomers; AIM method; SPINSPIN keyword.

Introduction

Purine and pyrimidine ring systems form the backbone of many important biological molecules, such as nucleic acids, cofactors and various toxins. The ability of these molecules to interact with proteins has been extensively exploited in the preparation of inhibitors specific against certain conditions,   such as Gleevee (cancer) or aronixil (atherosclerosis), for example. The privileged nature of the purine/pyrimidine structure in terms of their shape and hydrogen-bonding characteristics make them ideal starting points in the search for new chemical entities of biological significance [1]. The synthesis and chemistry of purine has attracted considerable attention due to its pharmaceutical and biological properties. Some purine derivatives such as theophylline have long been used as anti-inflammatory drugs and also in therapy for respiratory diseases such as asthma [2-4]. Phosphorus ylides are reactive systems, which take

part in many reactions of value in organic synthesis [5-15]. Several methods have been developed for the preparation of phosphorus ylides. These ylides are usually prepared by treatment of a phosphonium salt with a base, and phosphonium salts are usually obtained from the phosphine and an alkyl halide [5,9,10,12,13]. In recent years, there have been some reports about the synthesis of stable phosphorus ylides [16-20].

In continuation of our current interest in the development of new approaches to heterocyclic and carbocyclic systems, the kinetics and mechanistic study along with theoretical calculations of a facile, synthesis of the reaction between triphenylphosphine **1**, dialkyl acetylenedicarboxylates **2** and theophylline **3** (as a protic/nucleophilic reagent) were investigated for generation of phosphorus ylides **4a-c** involving the two geometrical isomers such as *Z*- and *E*- isomers. Synthesis of which was earlier reported [21]. For assignment of the two Z and E isomers as a major or minor form in phosphorus ylides **4a-b** containing a

---

*Corresponding author. Tel: +(98) 5412446565; Fax: +(98) 5412446565; E-mail: smhabibi_usb@yahoo.com

theophylline, first the *Z*- and the E- isomers were optimized for all ylide structures at HF/6-31G(d,p) level of theory by Gaussian03 package program. The relative stabilization energies of both the geometrical isomers have been calculated at B3LYP/6-311++G** level. Atoms in molecules (AIM) and natural population analysis (NPA) methods and CHelpG keyword at HF/6-31G(d,p) level of theory have been performed in order to gain a better understanding of the most geometrical parameters of both the E-**4(a,b)** and the *Z*-**4(a,b)** of phosphorus ylides. The numbers of critical points and intramolecular hydrogen bonds as well as the charge of atoms that constructed on the *Z*- and E- isomers have been recognized. The results altogether reveal the effective factors on stability of *Z*- and E- ylide isomers. In addition, J_{x-y}, the values of proton and carbon coupling constants and also chemical shifts (δ^H_{iso}, δ^C_{iso}) have been calculated at mentioned level using SPINSPIN keyword

Results and discussion

Recently, different reports have been published on the synthesis of stable phosphorus ylides from the reaction between triphenylphosphine and reactive acetylenic esters in the presence of N-H, C-H or S-H heterocyclic compounds. These ylides usually exist as a mixture of the two geometrical isomers, although some ylides exhibit one geometrical isomer. Assignment of the stability of the two *Z*- and E- isomers is possible in phosphorus ylides by experimental methods such as ^{1}H and ^{13}CNMR and IR spectroscopies, mass spectrometry and elemental analysis data. For this reason quantum mechanical calculation has been performed in order to gain a better understanding of the most important geometrical parameters and also relative energies of both the geometrical isomers.

Calculations

In order to determine more stable form of both the geometrical isomers [*Z*-**4(a, b)** and E-**4(a, b)**] of ylides (**4a** or **4b**), which is shown in Fig. **1**, first their structures were optimized at HF/6-31G(d,p) level of theory [22] by Gaussian03 package program [23]. Also relative stabilization energy of the two isomers have been calculated at HF/6-31G(d,p) and B3LYP/6-311++G** levels (See Figs. **2** and **3**). The relative stabilization energies for the two [*Z*-**4(a, b)** and E-**4(a, b)**] isomers are reported in Table **1**, as can be seen, *Z*-**4a** and *Z*-**4b** isomers are more stable than E-**4a** and E-**4b** forms (1.03 and 1.69 kcal/mol, respectively) at B3LYP level.

Further investigation was undertaken in order to determine more effective factors on stability of the two *Z*- and E- isomers on the basis of AIM calculations

[24] at HF/6-31G(d,p) level of theory by the AIM2000 program package [25].
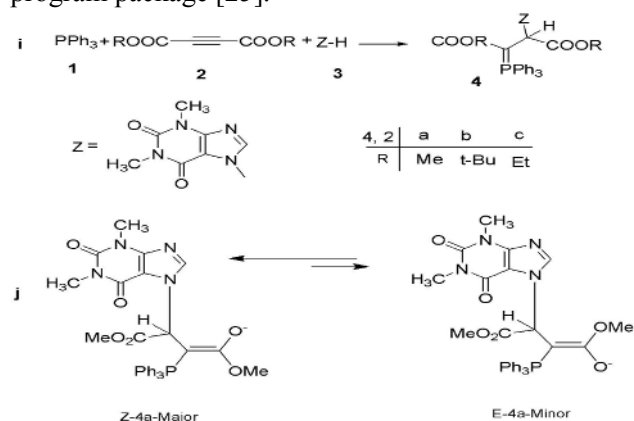
Fig. 1: The reaction between triphenylphosphine 1, dialkyl acetylenedicarboxylate 2 (2a or 2b) and theophylline 3 for generation of stable phosphorus ylides 4 (4a or 4b). U) The two isomers Z-4a and E-4a (major and minor, respectively) of ylide 4a.

Table 1: The relative energy (kcal/mol) for both the *Z*- and *E*- isomers of ylides 4a and 4b, obtained at HF/6-31G (d,p) and B3LYP/6-3ll++G(d,p) levels.

Geometrical isomer	HF	B3LYP
Z-4a	1.50	1.03
E-4a	0.00	0.00
Z-4b	1.93	1.69
E-4b	0.00	0.00
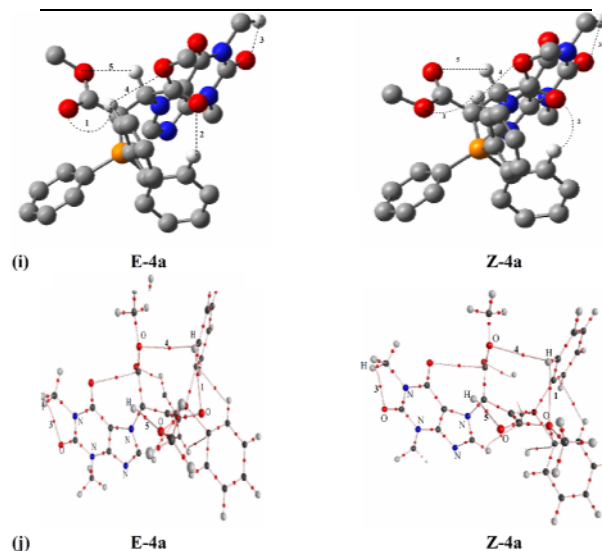
Fig.2 (i) Intermolecular hydrogen bonds (dotted lines) in the two *E*-**4a** and *Z*-**4a** geometrical isomers of stable ylide **4a**. **(j)** A part of molecular graphs, including intermolecular hydrogen bond critical points (BCPS) for the two rotational isomers such as *E*-**4a** and *Z*-**4a**. Small red spheres and lines corresponding to BCPS bond paths, respectively.

(i)   E-4b   Z- 4b

(j)   E-4b   Z-4b
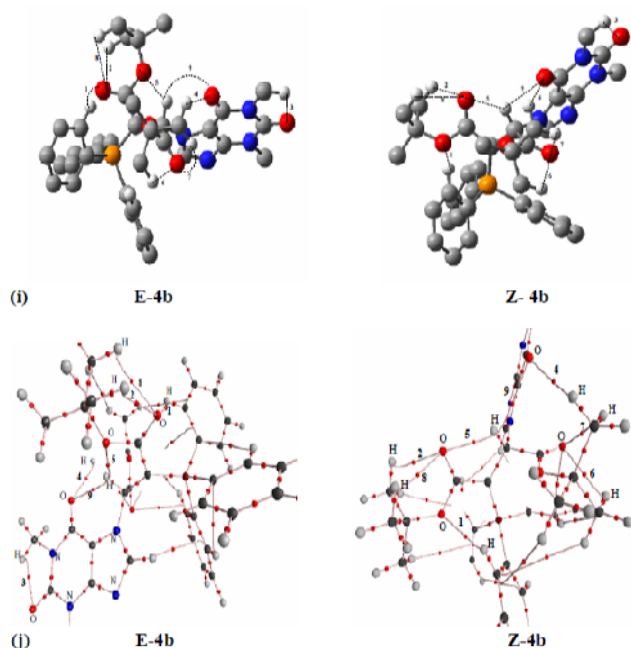
Fig. 3: (i) Intermolecular hydrogen bonds (dotted lines) in the two *E-4b* and *Z-4b* geometrical isomers of stable ylide **4b**. **(j)** A part of molecular graphs, including intermolecular hydrogen bond critical points (BCPS) for the two rotational isomers such as *E-4b* and *Z-4b*. Small red spheres and lines corresponding to BCPS bond paths, respectively.

In recent years, AIM theory has often applied in the analysis of H-bonds. In this theory, the topological

properties of the electron density distribution are derived from the gradient vector field of the electron density $\nabla\rho(r)$ and on the Laplacian of the electron density $\nabla^2\rho(r)$. The Laplacian of the electron density, $\nabla^2\rho(r)$, identifies regions of space wherein the electronic charge is locally depleted [$\nabla^2\rho(r) > 0$] or built up [$\nabla^2\rho(r) < 0$] [24]. Two interacting atoms in a molecule form a critical point in the electron density, where $\nabla\rho(r) = 0$, called the bond critical point (BCP). The values of the charge density and its Laplacian at these critical points give useful information regarding the strength of the H-bonds [25]. The ranges of $\rho(r)$ and $\nabla^2\rho(r)$ are $0.002 - 0.035$ e/a_0^3 and $0.024 - 0.139$ e/a_0^5, respectively, if H-bonds exist [26]. The AIM calculation indicates intramolecular hydrogen bond critical points (H-BCP) for the two *Z-4*(**a**, **b**) and *E-4*(**a**, **b**) isomers. Intramolecular H-BCPs along with a part of molecular graphs for the two rotational isomers are shown in Figures **2** and **3** (dotted line). Most important geometrical parameters involving some H-bonds (bond length and their relevant bond angle) are reported in Table **2**. The electron density $(\rho)\times10^3$, Laplacian of electron density $\nabla^2\rho(r)\times10^3$, and energy density $-H(r)\times10^4$ are also reported in Table **3**.

Table 2: Most important rotational parameters corresponding to H-bonds (bond lengths and their relevant angles) for the two *Z* and *E* isomers in both ylides 4a and 4b. Bond lengths in Angstroms and bond angles in degrees, respectively.

	E-4a		Z-4a
CnH26·.. 042	2.49a (127.24)b	CnH26·.. 043	2.64a (118.48)b
C32H3s... *Os*	2.28 (125.54)	C32H3s... *Os*	2.34 (118.17)
C6sH71... 063	2.23 (105.01)	C6sH71... 063	2.23 (105.46)
	E-4b		Z-4b
C6sH69... 042	2.43a (111.43)b	C6sH69... 042	2.41a(111.88)b
CsoHs9...*Os4*	2.82 (124.47)	CsoHs9...*Os4*	2.73 (123.00)
C79Hs4…*Os*	2.52 (110.99)	C79Hs4…*Os*	2.52 (111.04)
a bond length	b bond angle		

Table 3: The values of a=p x10^3, b=V^2 p x10^3 and c=-H(r) x10^4 for both the Z-4(a,b) and E-4(a,b) isomers ofylide 4a and 4b calculated at the hydrogen bond critical points. All quantities are in atomic units.

E	a	b	c	Z	a	b	c
1	11.25"(9.82)b	42.6a(37.56)b	9.98"(9.95)b	1	8.52"(7.51)b	34.96a(30.92)b	12.63"(11.62)b
2	12.61(14.25)	48.32(52.44)	12.62(9.45)	2	13.12(13.18)	50.16(50.32)	12.65(12.47)
3	19.73(19.54)	89.08(89.60)	26.18(27.40)	3	19.71(19.64)	89.00(89.08)	26.16(26.51)
4	4.35(3.51)	18.28(15.00)	8.87(7.95)	4	5.33(4.47)	22.00(19.16)	9.60(9.90)
5	20.24(19.91)	86.48(84.36)	19.53(18.48)	5	20.43(19.28)	91.84(89.08)	24.32(27.01)

6	10.70	41.76	12.49	6	10.73	41.84	12.44
7	11.59	45.76	14.12	7	11.61	45.84	14.15
8	12.76	48.44	11.91	8	13.11	49.96	12.29
9	9.46	37.48	11.93	9	8.63	35.2	12.50

[a] are relevant to the two E-4a and Z-4a isomers, respectively.
[b] are relevant to the two *E-4b* and Z-4b isomers, respectively.

A negative total energy density at the BCP reflects a dominance of potential energy density, which is the consequence of accumulated stabilizing electronic charge [27]. Herein, the number of hydrogen bonds in both categories (*E*-**4a** and *Z*-**4a**) and (*E*-**4b** and *Z*-**4b**) are (5 and 5) and also (9 and 9) respectively. The values of ρ and $\nabla^2\rho(r)$ for those are in the ranges (0.003 – 0.020 and 0.004 – 0.019 e/a_0^3) and (0.004 – 0.020 and 0.005 – 0.020 e/a_0^3) and also (0.015 – 0.089 and 0.019 – 0.089 e/a_0^5) and (0.018– 0.089 and 0.022– 0.091 e/a_0^5), respectively. In addition, the Hamiltonian [-H(r) $\times 10^4$] are in the ranges (7.95 – 27.40 and 9.90 – 27.01 au) and (8.87 – 26.18 and 9.60 – 26.16 au), respectively (see Table **3**). These HBs show $\nabla^2\rho(r) > 0$ and H(r) < 0, which according to classification of Rozas et al. [28] are medium-strength hydrogen bonds. In both ylides (see Table **4**) the dipole moment for the two *E*-**4a** and *E*-**4b** isomers (7.82 and 8.53 D) are smaller than the two *Z*-**4a** and *Z*-**4b** isomers (11.46 and 12.15 D,

respectively) and the value of -H_{tot} (=$\sum$-H(r) $\times 10^4$) for the two *E*-**4a** and *E*-**4b** isomers (73.25 and 127.66 au) are smaller than the two *Z*-**4a** and *Z*-**4b** isomers (87.52 and 136.77 au, respectively). Although, dipole moments in both the *Z*-**4**(**a**, **b**) are more than the *E*-**4**(**a**, **b**) and appear as an effective factor on instability of the *Z*-**4**(**a**, **b**), but the values of -H_{tot} in the *Z*-**4**(**a**, **b**) are larger than *E*-**4**(**a**, **b**) as an important fact on stability of *Z*-**4**(**a**, **b**). It seems that stability on both the *Z*-**4**(**a**, **b**) stem from the two opposite factors (dipole moment and the total Hamiltonian) in which the influence of the total Hamiltonian is superior to that of dipole moment. Difference of -H_{tot} between the *Z*-**4a** and the *E*-**4a** (14.27 au) and also *Z*-**4b** and *E*-**4b** (9.11 au) as a stability factor are larger than difference of dipole moment between the *Z*-**4a** and *E*-**4a** (3.64 D) and also the *Z*-**4b** and *E*-**4b** (3.62 D) as a instability factor, hence, effect of –H(r) is dominated on influence of dipole moment in the *Z*-**4**(a,b) category.

Table 4: The most important geometrical parameters involving the value of H_{101}/au, dipole moment/D and the number of hydrogen bonds for the two *Z*- and *E*- isomers of ylides 4a and 4b.

Geometrical isomer	H_{101}/au	dipole moment/D	number of hydrogen bond
E-4a	73.25	7.82	5
Z-4a	87.52	11.46	5
E-4b	127.66	8.53	9
Z-4b	136.77	12.15	9

As a result, *Z*-**4a** and *Z*-**4b** are stable isomers in comparison with the *E*-**4a** and *E*-**4b**. Although, on the basis of theoretical calculations (Table **1**), both the *E*-**4a** and *E*-**4b** have a slightly stability with respect to the two *Z*-**4a** and *Z*-**4b** (1.03 and 1.69 kcal/mol, respectively) isomers and seems to be different from the results of predictable properties of the most important geometrical parameters. Perhaps, this slightly different behavior is relevant to the huge structures of the two ylides **4**(**a**,**b**) involving three large atoms such as the oxygen, nitrogen and phosphorus and the large number of other atoms (C and H). This point, made a limitation in application of basis set higher than HF/6-31G(d,p) in a higher performance to gain more accurate calculations. Nevertheless, the

results involving the large different of -H_{tot} as a dominate factor of stability over the small different of dipole moment as a instability factor in the *Z*-**4**(**a**, **b**) category, are compatible with the experiment results from the ^{1}H, ^{13}C, ^{31}P NMR spectroscopes [21] wich indicate the two isomers of *Z*-**4a** and *Z*-**4b** with the experimental abundance percentage of 53 and 95 (major forms) with respect to the *E*-**4**(**a**, **b**) (minor forms).

Also, the charge on different atoms which are calculated by atoms in molecules (AIM) and natural population analysis (NPA) methods and also CHelpG keyword at HF/6-31G(d,p) level are reported in Table **5** for the two *Z*- and *E*- isomers of ylides **4a** and **4b**.

There is good agreement between the results in three methods.

The individual chemical shifts have been characterized by NMR calculations at mentioned level using SPINSPIN keyword. The total spin-spin coupling constant is the sum of four components: the paramagnetic spin-orbit (PSO), diamagnetic spin-orbit (DSO), Fermi-contact (FC) and spin-dipole (SD) terms. The value of chemical shifts (δ) and coupling constants (J_{x-y}) are reported in (Tables **6-9**) for the two minor *E*-**4**(**a**, **b**) and major *Z*-**4**(**a**, **b**) geometrical isomers. As can be seen, there is good agreement between both the experimental [21] and theoretical chemical shifts (δ) and coupling constants (J_{x-y}). In the present work, molecular structures of ylides **4a-b** involving large atoms such as six oxygen atoms, one phosphorus and four nitrogen atoms are huge along with the large numbers of other atoms, for this reason, employment of higher level of theory with basis set higher than HF/6-31G(d,p) is impossible for a higher performance to gain more accurate calculations. This limitation causes a small difference between both the experimental and theoretical coupling constants in some functional groups.

Table 5: The charges on different atoms for the two *Z* and *E* isomers in both ylides **4a** and **4b** calculated by AIM, NBORead and CHelpG methods, respectively at HF/6-31G(d,p) theoretical level.

number of atom	*Z*-**4a**	*E*-**4a**	*Z*-**4b**	*E*-**4b**
C1	0.67[a]	0.71	0.71	0.75
	0.09[b]	0.08	0.07	0.06
	0.09[c]	0.08	0.07	0.06
C6	-8.09×10^{1}	-7.95×10^{1}	-7.50×10^{1}	-7.46×10^{1}
	-0.66	-0.65	-0.63	-0.63
	-0.66	-0.65	-0.63	-0.63
C7	1.89	1.88	1.91	1.89
	0.87	0.87	0.90	0.90
	0.87	0.87	0.90	0.90
O42	-1.38	-1.40	-1.40	-1.41
	-0.64	-0.66	-0.65	-0.68
	-0.64	-0.66	-0.65	-0.68
O43	-1.27	-1.27	-1.29	-1.27
	-0.67	-0.65	-0.73	-0.71
	-0.67	-0.65	-0.73	-0.71
P8	3.21	3.21	3.21	3.21
	1.24	1.23	1.23	1.23
	1.24	1.23	1.23	1.23

[a] Calculated by AIM method.
[b] Calculated by NBORead method.
[c] Calculated by CHelpG method.

Table 6: Selected ^{1}H NMR chemical shift (δ in ppm) for some functional groups in the *E*-**4a** isomer as a minor form.

groups	δ^{H}/ppm
6H, 2s, 2 OMe	3.56-3.64[a] (3.10-3.47)[b]
1H, d, P=C-CH	5.50 (5.59)
1H, s, N=C-H	8.16 (7.17)
15H, m, 3C$_6$H$_5$	7.40-7.71(7.35-7.74)

[a] Experimental data in accord with the results reported in the literature.
[b] Theoretical data.

Table 7: Selected ^{1}H NMR chemical shift (δ in ppm) and coupling constants (J in Hz) for some functional groups in the *Z*-**4a** isomer as a major form.

groups	δ^{H}/ppm	J_{PH} /Hz
6H, 2s, 2 Me	3.18-3.61[a] (3.20-3.46)[b]	
1H, d, P=C-CH	5.53 (5.94)	17.6(24.7)

1H, s, N=C-H	8.28(7.35)	
15H, m, 3C$_6$H$_5$	7.40-7.71(7.48-7.72)	

[a] Experimental data in accord with the results reported in the literature.
[b] Theoretical data.

Table 8: Selected ^{13}C NMR chemical shift (δ in ppm) and coupling constants (J in Hz) for some functional groups in the *E*-**4a** isomer as a minor form.

groups	δ^C/ppm	J$_{PC}$/Hz
d, P-C-CH	60.1[a](55.31)[b]	15.8(14.30)
C$_8$H$_9$N$_4$O$_2$	141.1(137.83)	
d, C$_{ipso}$ of 3C$_6$H$_5$	125.2(126.4)	91.0(94.48)
d, C$_{meta}$ of 3C$_6$H$_5$	129.0(126.0)	
C$_{para}$ of 3C$_6$H$_5$	132.5(131.9)	
d, C$_{ortho}$ of 3C$_6$H$_5$	133.4(132.9)	8.8(10.95)
d, P-C=C	170.5(168.16)	
d, C=O$_{ester}$	170.9(169.2)	

[a] Experimental data in accord with the results reported in the literature.
[b] Theoretical data**.**

Table 9: Selected ^{13}C NMR chemical shift (δ in ppm) and coupling constants (J in Hz) for some functional groups in the *Z*-**4a** isomer as a major form.

groups	δ^C/ppm	J$_{PC}$/Hz
d, P-C-CH	60.1[a](56.25)[b]	
C$_8$H$_9$N$_4$O$_2$	139.9(137.53)	
d, C$_{ipso}$ of 3C$_6$H$_5$	125.9(126.5)	88.7(92.5)
d, C$_{meta}$ of 3C$_6$H$_5$	129.0(126. 6)	
C$_{para}$ of 3C$_6$H$_5$	132.5(131.8)	
d, C$_{ortho}$ of 3C$_6$H$_5$	133.4(133.9)	8.8(10.9)
d, P-C=C	170.3(165.2)	
d, C=O$_{ester}$	170.9(169.4)	

[a] Experimental data in accord with the results reported in the literature.
[b] Theoretical data.

Kinetics Studies

To gain further insight into mechanism in reaction between triphenylphosphin **1,** dialkyl acetylenedicarboxylates **2** and theophylline **3** (as a protic/nucleophilic reagent) for generation of phosphorus ylids **4a-b,** a kinetics study of the reactions was undertaken by UV spectrophotometeric technique. Synthesis of these reactions has been reported earlier [21]. First, it was necessary to find the appropriate wavelength to follow the kinetic study of the reaction. For this purpose, in the first experiment, 3×10^{-3} mol.L^{-1} solution of compounds **1, 2b** and **3** was prepared in 1,4-dioxane as solvent. An approximately 3 mL aliquot from each reactant was pipetted into a 10 mm light path quartz spectrophotometer cell, and the relevant spectra were recorded over the wavelength range 200-400 nm. Figures **4**, **5** and **6** show the ultraviolet spectra of compounds **1**, **2b** and **3** respectively. In a second experiment, a 1mL aliquot from the 3×10^{-3} mol.L^{-1} solutions of each compound of **1** and **3** was pipetted first into a quartz spectrophotometer cell (as there is no reaction between them), later 1mL aliquot of the 3×10^{-3} mol.L^{-1} solution of reactant **2b** was added to the mixture and the reaction monitored by recording scans of the entire spectra every 12 min over the whole

reaction time at ambient temperature. The ultra-violet spectra shown in Fig. **7** are typical for generation of ylide **4b**. From this, the appropriate wavelength was found to be 330 nm (corresponding mainly to product **4b**). Since at this wavelength, compounds **1**, **2b** and **3** have relatively no absorbance value. This, then provided the opportunity to fully investigate the kinetics of the reaction between triphenylphosphine **1**, di-*tert*-butyl acetylenedicarboxylate **2b** and theophylline **3** at 330 nm in the presence of 1,4-dioxane as solvent. Since the spectrophotometer cell of the UV instrument had a 10-mm light-path cuvette, the UV-vis spectra of compound **4b** were measured over the concentration range (2×10^{-4} mol.L^{-1} $\leq$ M$_{4c}$ $\leq 10^{-3}$ mol.L^{-1}) to check for a linear relationship between absorbance values and concentrations. With the suitable concentration range and wavelength identified, the following procedure was employed.
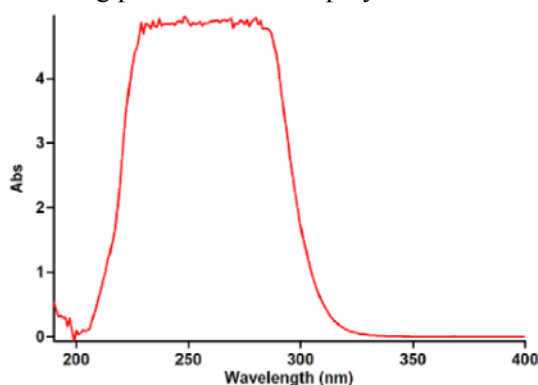
Figure 4: The UV spectrum of 10^{-3} mol.L^{-1} triphenylphosphine 1 in 1,4-dioxane.
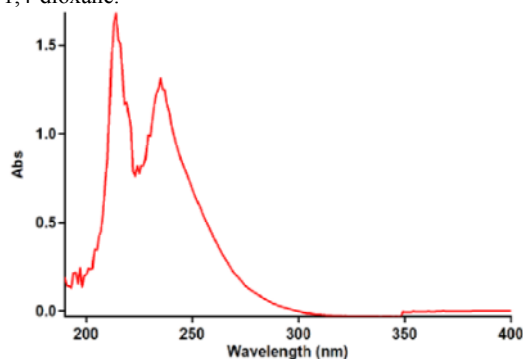
Figure 5: The UV spectrum of 10^{-3} mol.L^{-1} di-*tert*-butyl-acetylenedicarboxylate **2c** in 1,4-dioxane.

For each kinetic experiment, first a 1mL aliquot from each freshly made 3×10^{-3} mol.L^{-1} solution of compounds **1** and **3** in 1,4-dioxane was pipetted into a quartz cell, and then a 1mL aliquot of the 3×10^{-3} mol.L^{-1} of solution of reactant **2b** was added to the mixture, keeping the temperature at 15.0ºC. The reaction kinetics was followed by plotting UV absorbance against time.
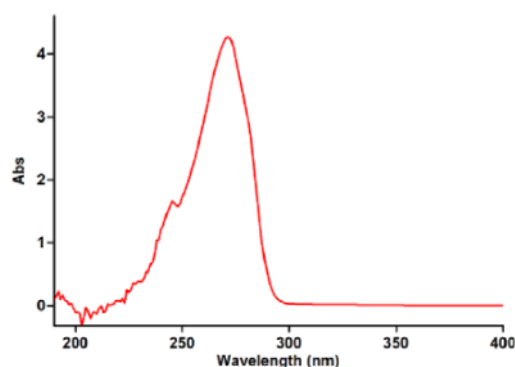
Figure 6: The UV spectrum of 10^{-3} mol.L^{-1} theophylline **3** in 1,4-dioxane.
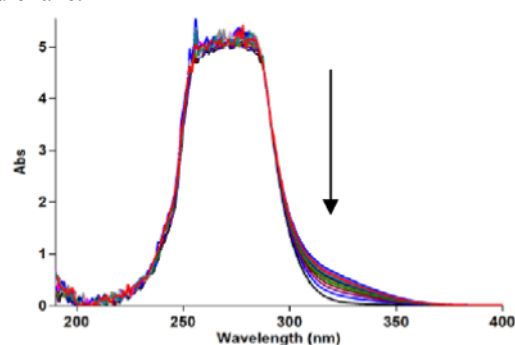
Figure 7: The UV spectra of the reaction between 1,2b and 3 with 10^{-3} mol.L^{-1} concentration of each compound proceeds in 1,4-dioxane with 10 mm light-path cell for generation of ylide 4b.

Fig. **8** shows the absorbance change (dotted line) versus time for the 1:1:1 addition reaction between compounds **1**, **2b** and **3** at 15.0ºC. The infinity absorbance (A$_\infty$) that is the absorbance at reaction completion, can be obtained from Fig. **8** at t =103 min. With respect to this value, zero, first or second curve fitting could be drawn automatically for the reaction by the software [29] associated with the UV instrument. Using the original experimental absorbance versus time data provided a second-order fit curve (full line) that fits exactly the experimental curve (dotted line) as shown in Fig. **9**. Thus, the reaction between triphenylphosphine **1**, di-*tert*-butyl acetylenedicarboxylate **2b** and **3** follows second-order kinetics. The second-order rate constant (k_2) is then automatically calculated using a standard equation [29] within the program at 15.0ºC. It is reported in Table **10**.

Furthermore Furthermore, kinetic studies were carried out using the same concentration of each reactant in the continuation of experiments with concentrations of 5×10^{-3} mol.L^{-1} and 7×10^{-3} mol.L^{-1} respectively. As expected, the second-order rate constant was independent of concentration and its

value was the same as in the previous experiment. In addition, the overall order of reaction was also 2.
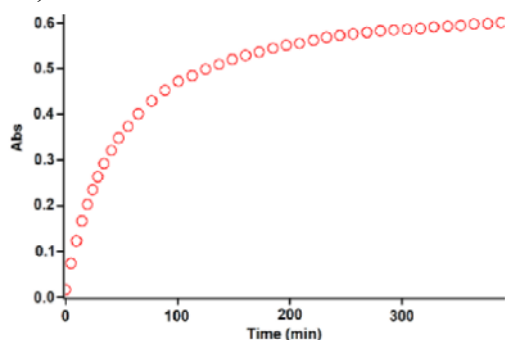
Figure 8: The experimental absorbance changes (dotted line) against time at 330 nm for the reaction between compounds 1,2b and 3 at 15.0 °C.
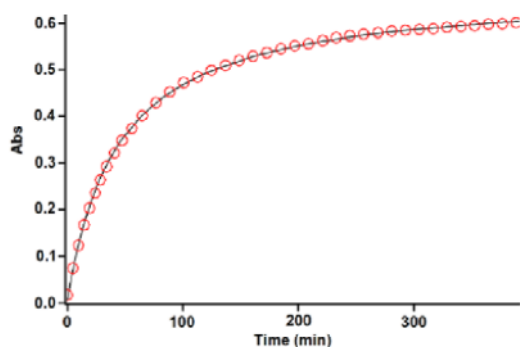
Figure 9: Second order fit curve (full line) accompanied by the original experimental curve (dotted line) for the reaction between compounds **1,2b** and **3** at 330 nm and 15.0 °C in 1,4-dioxane.

Effect of solvents and temperature

To determine the effect of change in temperature and solvent environment on the rate of reaction, it was elected to perform various experiments at different temperatures and solvent polarities but otherwise under the same conditions as for the previous experiment. For this purpose, 1,2-dichloroethane with 10 dielectric constant was chosen as a suitable solvent since it is not only could be dissolved all compounds but also did not react with them. The effects of solvents and temperature on the rate constant are given in Table **10**. The results show that the rate of reaction in each case was increased at higher temperature. In addition, the rate of reaction between **1**, **2b** and **3** was accelerated in a higher dielectric constant environment (1,2-dichloroethane) in comparison with a lower dielectric constant environment (1,4-dioxane) at all temperatures investigated. In the temperature range studied, the dependence of the second-order rate constant (Ln k_2) of the reactions on reciprocal temperature is consistent with the Arrhenius equation, giving activation energy

of reaction between **1**, **2b** and **3** (24.9 kJ/mol) from the slope of Figure **10**.

Effect of concentration

To determine reaction order with respect to triphenylphosphine **1** and dialkyl acetylene-dicarboxylate 2 (2b), in the continuation of experiments, all kinetic studies were carried out in the presence of excess 3. Under this condition, the rate equation may therefore be expressed as:

$$rate = k_{obs}[1]^{\alpha}[2]^{\beta} \quad k_{obs} = k_2[3]^{\gamma} \qquad \text{or}$$

$$Ln\, k_{obs} = Ln\, k_2 + \gamma\, Ln[3] \qquad (1)$$

In this case (3×10^{-2} mol.L^{-1} of **3** instead of 3×10^{-3} mol.L^{-1}) using the original experimental absorbance versus time data provides a second order fit curve (full line) against time at 330 nm which exactly fits the experimental curve. The value of rate constant was the same as that of obtained from the previous experiment (3×10^{-3} mol.L^{-1}). Repetition of the experiments with 5×10^{-2} mol.L^{-1} and 7×10^{-2} mol.L^{-1} of **3** gave, separately, the same fit curve and rate constant. In fact, the experimental data indicated that the observed pseudo second order rate constant (k_{obs}) was equal to the second order rate constant (k_2), this is possible when γ is zero in equation (1). It is appears, therefore, that the reaction is zero and second order with respect to **3** (as a protic/nucleophilic reagent) and the sum of **1** and 2 (**2b**) ($\alpha + \beta = 2$), respectively. To determine reaction order with respect to dialkyl acetylenedicarboxylate 2 (**2b**), the continuation of experiment was performed in the presence of excess of **1** (rate $= k'_{obs}[3]^{\gamma}[2]^{\beta}$, $k'_{obs} = k_2[1]^{\alpha}$ (2)). The original experimental absorbance versus time data and provide a pseudo first order fit curve at 330 nm, which exactly fits the experimental curve (dotted line) as shown in Figure **11**.

As a result since $\gamma = 0$ (as determined previously), it is reasonable to accept that the reaction is first order with respect to compound 2 (**2b**) ($\beta = 1$). Because the overall order of reaction is 2 ($\alpha + \beta + \gamma = 2$) it is obvious that $\alpha = 1$ and order of triphenylphosphine **1** must be equal to one. This observation was obtained also for reactions between (**1, 2c** and **3**) and (1, **2a** and **3**). Based on the above results, a simplified proposed reaction mechanism is shown in Figure **12**.

The experimental results indicate that the third step (rate constant k3) is possibly fast. In contrast, it may be assumed that the third step is the rate determining step for the proposed mechanism. In this case the rate law can be expressed as follows:

$$rate = k_3[I_1][3] \qquad (3)$$

Table 10: values of overall second order rate constant for the reactions between (1,2a and 3), (1,2b and 3) and (1,2c and 3) in the presence of solvents such as 1,2-dichloroethane and 1,4-dioxane, respectively, at all temperatures investigated.

Reactions	Solvent	ε	k_2. mol^{-1}.L.min^{-1}			
			15.0 ^{o}C	20.0 ^{o}C	25.0 ^{o}C	30.0 ^{o}C
1,2a and **3**	1,4-dioxane	2	457.1	491.4	556.7	628.7
1,2a and **3**	1,2-dichloroethane	10	496.2	545.1	610.4	681.3
1,2c and **3**	1,4-dioxane	2	316.9	350.1	392.0	452.5
1,2c and **3**	1,2-dichloroethane	10	350.4	385.9	430.7	492.0
1,2b and **3**	1,4-dioxane	2	60.4	72.0	84.3	101.7
1,2b and **3**	1,2-dichloroethane	10	69.6	82.5	96.0	113.7
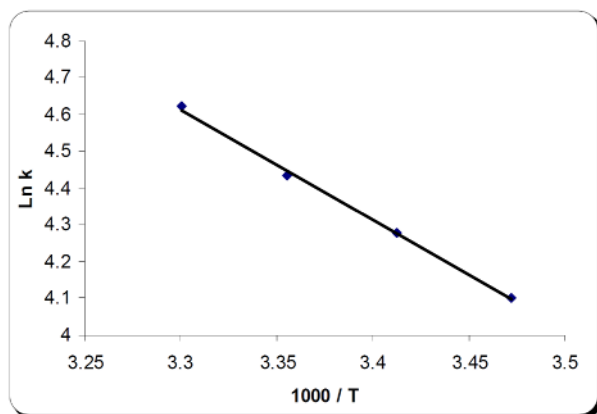
Figure 10: Dependence of second order rate constant (Ln k_2) on reciprocal temperature for the reaction between compounds **1,2b** and **3** measured at wavelength 330 nm in 1,4-dioxane in accordance with Arrhenius equation.
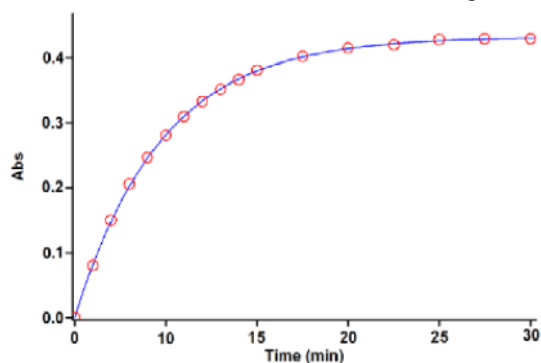
Figure 11: Pseudo first order fit curve (full line) accompanied by the original experimental curve (dotted line) for the reaction between 2b and 3 in the presence of axcess 1 (10^{-2} mol.L^{-1}) at 330 nm and 15.0^{o}C in 1,4-dioxane.

The steady state assumption can be employed for [I$_1$] which is generated following equation,

$$[I_1] = \frac{k_2[1][2]}{k_{-2} + k_3[3]}$$

The value of [I$_1$] can be replaced in equation (3) to obtain this equation:

$$rate = \frac{k_2 k_3 [1][2][3]}{k_{-2} + k_3 [3]}$$

Since it was assumed that *k3* is relevant to the rate determining step, it is reasonable to make the following assumption: *k2 >> k3*   [3]

So the rate of low becomes:

$$rate = \frac{k_2 k_3 [1][2][3]}{k_{-2}}$$

The final equation is indicates that overall order of reaction is three which is not compatible with experimental overall order of reaction (=two). In addition, according to this equation, the order of reaction with respect to theophylline **3** is one, whereas it was actually shown to be equal to zero. For this reason, it appeared that the third step is fast. If we assume that the fourth step (rate constant k_4) is the rate-determining step for the proposed mechanism, in this case, there are two ionic species to consider in the rate determining step, namely phosphonium ion (I$_2$) and theophylline (Z$^-$). The phosphonium and theophylline ions, as we see in Fig.**12**, have full positive and negative charges and form very powerful ion- dipole bonds to the 1, 2-dichloroethane, the high dielectric constant solvent. However, the transition state for the reaction between two ions carries a dispersed charge, which here is divided between the attacking theophylline and the phosphonium ions. Bonding of solvent (1, 2-dichloroethane) to this dispersed charge would be much weaker than to the concentrated charge of theophylline and phosphonium ions. The solvent thus stabilize the species ions more than it would the transition state, and therefore E$_a$ would be higher, slowing down the reaction. However, in practice, 1, 2-dichloroethane speeds up the reaction (see Table **10**) and for this reason, the fourth step, which is independent of the change in the solvent medium, could not be the rate determining step. Furthermore, the rate law of formation of the product (fourth step) for a proposed reaction mechanism with application

of steady state assumption can be expressed by:

rate = $k_4 [I_2] [Z]$

By application of steady state for $[I_2]$ and $[Z^-]$, and replacement of their values   in the above equation, the following equation is obtained:

This equation is independent of rate constant for the fourth step (k_4) and shows why the fourth step would not be affected by a change in the solvent medium. In addition, it has been suggested earlier that the kinetics of ionic species' phenomena (e.g., the fourth step) are very fast [30-32].
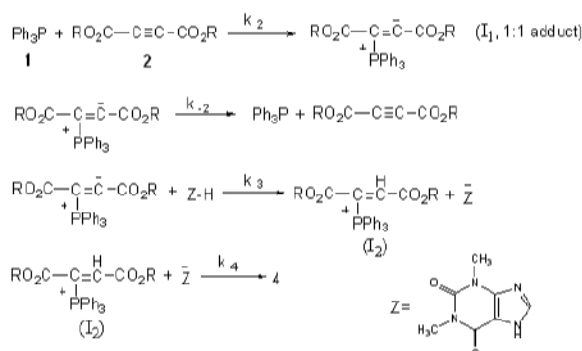
Figure 12: proposed mechanism for the reaction between 1,2 (2a, 2b or 2c) and 3 on the basis of litratures for

$$rate = \frac{k_2 k_3 [1][2][3]}{k_{-2} + k_3 [3]}$$

generation of phosphorus ylides 4 (4a, 4b or 4c).

If the first step (rate constant k_2) were the rate determining step, in this case, two reactants (triphenylphosphine **1** and dialkyl acetylenedicarboxylate **2**), as we see in Figure **12**, have no charge and could not form strong ion-dipole bonds to the high dielectric constant solvent, 1,2-dichloroethane. However, the transition state carries a dispersed charge which here is divided between the attacking **1** and **2** and, hence, bonding of solvent to this dispersed charge is much stronger than the reactants, which lack charge. The solvent thus stabilizes the transition state more than it does the reactants and, therefore, E_a is reduced which speeds up the reaction. Our experimental results show that the solvent with higher dielectric constant exerts a power full effect on the rate of reaction (in fact, the first step has rate constant k_2 in the proposed mechanism) but the opposite occurs with the solvent of lower dielectric constant, (see Table **10**). The results of the current work (effects of solvent and concentration of compounds) have provided useful evidence for steps 1 (k_2), 3 (k_3) and 4 (k_4) of the reactions between triphenylphosphine **1**, dialkyl acetylenedicarboxylate **2** (**2a, 2b** or **2c**) and theophylline **3**. Two steps involving 3 and 4 are not determining, although the discussed

effects, taken altogether, are compatible with first step (k_2) of the proposed mechanism and would allow it to be the rate-determining step. However, a good kinetic description of the experimental result using a mechanistic scheme based upon the steady state approximation is frequently taken as evidence of its validity. By application of this, the rate formation of product **4** from the reaction mechanism (Fig. **12**) is given by:

$$\frac{d[4]}{dt} = \frac{d[ylide]}{dt} = rate = k_4 [I_2][Z^-] \quad (5)$$

We can apply the steady-state approximation to $[I_1]$ and $[I_2]$;

$$\frac{d[I_1]}{dt} = k_2 [1][2] - k_{-2} [I_1] - k_3 [I_1][3]$$

$$\frac{d[I_2]}{dt} = k_3 [I_1][3] - k_4 [I_2] [Z^-]$$

To obtain a suitable expression for $[I_2]$ to put into equation (5) we can assume that, after an initial brief period, the concentration of $[I_1]$ and $[I_2]$ achieve a steady state with their rates of formation and rates of disappearance just balanced. Therefore $d[I_1]/dt$ and $d[I_2]/dt$ are zero and we can obtain expressions for $[I_2]$ and $[I_1]$ as follows:

$$\frac{d[I_2]}{dt} = 0 \quad , \quad [I_2] = \frac{k_3 [I_1][3]}{k_4 [Z^-]} \quad (6)$$

$$\frac{d[I_1]}{dt} = 0 \quad , \quad [I_1] = \frac{k_2 [1][2]}{k_{-2} + k_3 [3]} \quad (7)$$

We can now replace $[I_1]$ in the equation (6) to obtain this equation:

$$[I_2] = \frac{k_2 k_3 [1][2][3]}{k_4 [Z^-][k_{-2} + k_3 [3]]}$$

The value of $[I_2]$ can be put into equation (5) to obtain   the   rate   equation   (8)   for   proposed mechanism:

$$rate = \frac{k_2 k_3 k_4 [1][2][3][Z^-]}{k_4 [Z^-][k_{-2} + k_3 [3]]} \quad \text{or} \quad rate = \frac{k_2 k_3 [1][2][3]}{[k_{-2} + k_3 [3]]}$$

(8)

Since experimental data were indicated that steps 3 (k3) and 4 (k4) are fast but step 1 (k2) is slow, it is therefore   reasonable   to   make   the   following assumption: $k_3 [3] >> k_{-2}$

So the rate equation becomes: $rate = k_2 [1][2]$ (9)

This equation which was obtained from a mechanistic scheme (shown in Fig. **12**) by applying the steady-state

approximation is compatible with the results obtained by UV spectrophotometery. With respect to the equation (9) that is shown overall reaction rate (Fig. **1**), the activation parameters involving $\Delta G^{\#}$, $\Delta S^{\#}$ and $\Delta H^{\#}$

Table 11: The activations parameters involving $\Delta G^{\#}$, $\Delta S^{\#}$ and $\Delta H^{\#}$ for the reactions between **1,2a** and **3,1,2b** and **3** and also **1,2c** and **3** at 15.0 °C in 1,4-dioxane.

reactions	$\Delta G^{\#}$ (kJ.mol^{-1})	$\Delta H^{\#}$ (kJ.mol^{-1})	$\Delta S^{\#}$ (kJ.mol^{-1})
1,2a and 3	81.4	10.8	-0.245
1,2c and 3	82.2	12.2	-0.243
1,2b and 3	86.1	20.1	-0.229
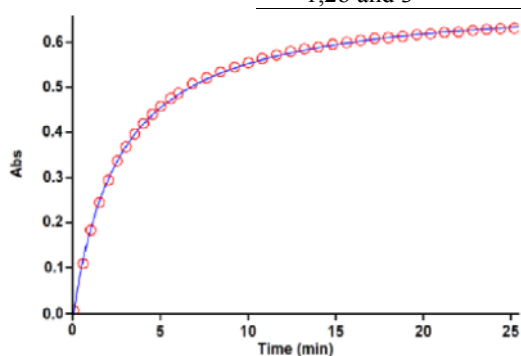
Figure 13: Second order fit curve (full line) accompanied by the original experimental curve (dotted line) for the reaction between compounds 1,2c and 3 at 330 nm and 15.0 °C in 1,4-dioxane.
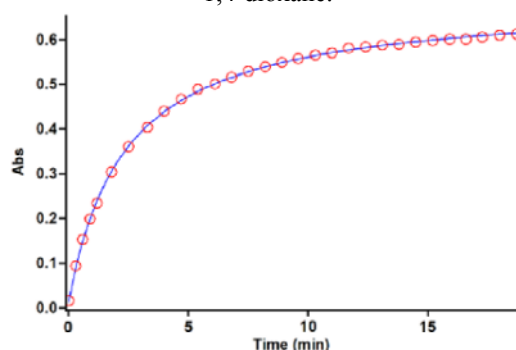
Figure 14: Second order fit curve (full line) accompanied by the original experimental curve (dotted line) for the reaction between compounds 1,2a and 3 at 330 nm and 15.0 °C in 1,4-dioxane.

Further kinetic investigations

To confirm the above observations, further experiments were performed with diethyl acetylenedicarboxylate **2c** and dimethyl acetylenedicarboxylate **2a**, respectively, under the same conditions used in the previous experiments. The values of the second-order rate constant (k_2) for the reactions between (**1, 2c** and **3**) and (**1, 2a** and **3**) are reported in Table **10**, for all solvents and temperatures investigated. The original experimental absorbance curves (dotted line) accompanied by the second order fit curves (full line), which exactly fit experimental curves (dotted line) (Figs. **13** and **14**) confirm the previous observations again for both reactions at 15.0°C and 330 nm.

As can be seen from Table **10** the behavior of diethyl acetylenedicarboxylate **2c** and dimethyl acetylenedicarboxylate **2a** is the same as for the di-*tert*-butyl acetylenedicarboxylate **2b** (Table **10**) with respect to the reaction with triphenylphosphine **1** and theophylline **3**. The rate of the former reactions was also accelerated in a higher dielectric constant environment and with higher temperatures; however, these rates under the same condition are approximately 7.1 to 7.5 times more than for the reaction with di-*tert*-butyl acetylenedicarboxylate **2b** (see Table **10**). It seems that both inductive and steric factors for the bulky alkyl groups in **2b** tend to reduce the overall reaction rate (see equation 9). In the case of dimetyl acetylenedicarboxylate **2a**, the lower steric and inductive effects of the dimethyl groups exert a powerful effect on the rate of reaction.

Conclusion

The assignment of the *Z*- and *E*- isomers as a minor or major form in both the ylides **4a** and **4b** was undertaken by atoms in molecules (AIM) and natural population analysis (NPA) methods and CHelpG keyword. Quantum mechanical calculation was clarified how the ylides **4a** and **4b** exist in solution as a mixture of the two geometrical isomers. This result was in good agreement with the experimental data. In addition, the NMR study on the basis of theoretical calculation were employed for determination of chemical shifts and coupling constants of the two major *Z*-**4**(**a**,**b**) and minor *E*-**4**(**a**,**b**) geometrical isomers and Kinetics investigation of the reactions was undertaken using UV spectrophotometry. The results can be summarized as follow: (1) the appropriate wavelengths and concentrations were determined to follow the reaction kinetics. (2) The overall reaction

order followed second-order kinetics and the reaction orders with respect to triphenylphosphine, dialkyl acetylenedicarboxylate and theophylline were one, one and zero respectively. (3) The values of the second-order rate constants of all reactions were calculated automatically with respect to the standard equation, using the software associated with the Cary-300 UV equipment. (4) The rates of all reactions were accelerated at higher temperatures. Under the same conditions, the activation energy for the reaction with di-*tert*-butyl acetylenedicarboxylate **2b** (24.9 kJ/mol) was higher than that for the both reactions which were followed by the diethyl acetylenedicarboxylate **2c** (17.0 kJ/mol) and dimethyl acetylenedicarboxylate **2a** (15.6 kJ/mol) in 1,2-dichloroethane (5) The rates of all reactions were increased in solvents of higher dielectric constant and this can be related to differences in stabilization by the solvent of the reactants and the activated complex in the transition state. (6) Increased steric bulk in the alkyl groups of the dialkyl acetylenedicarboxylates, accompanied by the correspondingly greater inductive effect, reduced the overall reaction rate. (7) With respect to the experimental data, the first step of proposed mechanism was recognized as a rate-determining step (k_2) and this was confirmed based upon the steady-state approximation. (8) Also, the third step was identified as a fast step (k_3). (9) The activation parameters involving $\Delta G^{\#}$, $\Delta S^{\#}$ and $\Delta H^{\#}$ were reported for the first step of three reactions.

Experimental

Quantum mechanical calculation has been performed by Gaussian03 program and using the AIM2000 program packages. Dialkyl acetylenedicarboxilate, triphenylphosphine and theophylline were purchased from Fulka (Buchs, Switzerland) and used without further purification. All extra pure solvents including 1,2-dichloroethane and 1,4-dioxane also obtained from Merk (Darmstadt, Germany). A Cary UV/Vis spectrophotometer model Bio-300 with a 10 mm light-path black quartz spectrophotometer cell was employed throughout the current work.

Acknowledgements

References

[1] Christiaan, W.; Westhuyzen, V.; Rousseau, A. L.; Parkinson, C. J. *Tetrahedron Lett.* **2007,** *63,* 5394.

[2] Smolensky, M. H.; Alonzo, G. E. Progress in the chronotherapy of nocturnal asthma, in: P.H.Redfern, B.Lemmer (Eds.), Physiology and Pharmacology of Biological Rhythms, Handbook of Pharmacology, Springer-Verlag, Heidelberg, **1997,** *125,* 205.

[3] Alonzo, G. E.; Cerocetti, J. G.; Smolensky, M. H.; *Chronobiol Int.,* **1999,** *16,* 663.

[4] Smolensky, M. H.; Lemmer, B.; Reinberg, A. E. *Advanced drug delivery reviews* **2007,** *59,* 852.

[5] Maryanoff, B. E.; Rietz, A. B.; Chem. Rev., **1989,** *89,* 863-927.

[6] Hudson, H. R., the Chemistry of "Organophosphorus Compound"s, Primary, Secondary, and Tertiary Phosphates and Heterocyclic Organophosphorus Compounds; Wiley: New York, **1990,** *I,* 386.

[7] Cherkasov, R. A.; Pudovik, M. A. *Russ. Chem. Rev.,* **1994,** *63,* 1019.

[8] Pietrusiewiz, K. M.; Zabloka, M. *Chem. Rev.,* **1994,** *94,* 1375.

[9] Kolodiazhnyi, O.; *Russ. Chem. Rev.* **1997,** *66,* 225.

[10] Yavari, I.; Baharfar, R. *Tetrahedron Lett.* **1998,** *9,* 1051.

[11] Ramazani, A; Bodaghi, A. *Tetrahedron Lett.* **2000,** *41,* 567.

[12] Maghsoodlou, M. T.; Habibi-khorassani, S. M.; Heydari, R.; Hassankhani, A; Marandi, G.; Nassiri, M.; Mosaddegh, E.; *Mol. Div.,* **2006,** *181,* 913.

[13] Yavari, I.; Hazeri, N.; Maghsoodlou, M. T.; Souri, S. *J. Mol. Cat,* **2007,** *264,* 313.

[14] Maghsoodlou, M. T.; Hazeri, N.; Habibi-Khorasani, S. M.; kakaei, R.; Nassiri, M., *Phosphorus,Sulfur and Silicon and the Relay. Elem.* **2006,** *181,* 25.

[15] Hazeri, N.; Habibi-Khorasani, S. M.; maghsoodlou, M. T.; Marandi, G.; Nassiri, M.; Shahzadeh, A. G. *J. Chem. Res.* **2006,** *4,* 215.

[16] Maghsoodlou, M. T.; Hazeri, N.; Habibi-Khorasani, S. M.; Shahzadeh, A. G.; Nassiri, M. *Phosphorus, Sulfur and Silicon and the Relay. Elem.,* **2006,** *181,* 913.

[17] Saghatforoush, L.; Maghsoodlou, M. T.; Aminkhani, A; Marandi, G.; Kabiri, R. *J. Sulfur. Chem.* **2006,** *27,* 583.

[18] Maghsoodlou, M. T.; Heydari, R.; Habibi-Khorasani, S. M.; Rofouei, M.; Nassiri, M.; Mosaddeg, E.; Hassankhani, A, *J. Sulfur. Chem,* **2006,** *27,* 341.

[19] Maghsoodlou, M. T.; Hazeri, N.; Afshari, G.; Niroumand, U., *Phosphorus, Sulfur and Silicon and the Relay. Elem.,* **2006,** *181,* 2681.

[20] Maghsoodlou, M. T.; Habibi-Khorasani, S. M.; Hazeri, N.; Nassiri, M.; kakaei, R.; Marandi, G.; *Phosphorus, Sulfur and Silicon and the Relay. Elem.,* **2006,** *181,* 553.

[21] Habibi-Khorassani, S. M.; Maghsoodlou, M. T.; Hazeri, N.; Bagherpour, Kh.; Rostamizadeh, M.; Najafi, H., *Phosphorus, Sulfur and Silicon and the Relay. Elem,* **(2010** Inpress).

[22] Reed, A. E.; Weinstock, R. B.; Weinhold, F. J., *J. Chem. Phys.* **1985,** *83,* 735.

[23] Frisch, M. J; Trucks, G. W.; Schlegel, H. B.; Scuseria, G. E.; Robb, M. A.; Cheeseman, J. R.; Zakrzewski, V. G.; Montgomery, J. A.; Stratmann, R. E.; Burant, J. C.; Dapprich, S.; Millam, J. M.; Daniels, A. D.; Kudin, K. N.; Strain, M. C.; Farkas, O.; Tomasi, J.; Barone, V.; Cossi, M.; Cammi, R.; Mennucci, B.; Pomelli, C.; Adamo, C.; Clifford, S.; Ochterski, J.; Petersson, G. A.; Ayala, P. Y.; Cui, Q.; Morokuma, K.; Malick, D. K.; Rabuck, A. D.; Raghavachari, K.; Foresman, J. B.; Cioslowski, J.; Ortiz, J. V.; Stefanov, B. B.; Liu, G.; Liashenko, A; Piskorz, P.; Komaromi, I.; Gomperts, R.; Martin, R. L.; Fox, D. J.; Keith, T.; Al-Laham, M. A.; Peng, C. Y.; Nanayakkara, A.; Gonzalez, C.; Challacombe, M.; Gill, P. M. W.; Johnson, B. G.; Chen, W.; Wong, M. W.; Andres, J. L.; Head-Gordon, M.; Replogle, E. S.; Pople, J. A.; Gaussian, Inc., Pittsburgh P. A, **2003.**

[24] Bader, R. F. W.; Atoms in Molecules: A Quantum Theory; Oxford Univ. New York, **1990.**

[25] Biegler konig, F. W.; Schonbohm, J.; Bayles, D.; *J. Comput. Chem.* **2001,** *22,* 545.

[26] Grabowski, S. J.; *J. Mol. Struct.* **2001,** *562,* 137.

[27] Arnold, W. D.; Oldfield, E. *J. Am. Chem. Soc.* **2000,** *122,* 1283.

[28] Rozas, I.; Alkorta, I., Elguero, J., *J. Am. Chem. Soc.* **2000,** *122,* 11154.

[29] Schwartz, L. M.; Gelb, R. I., *Anal. Chem.* **1978,** *50,* 1592.

[30] Wolff, M. A. *Chem. Instrum.* **1976,** *5,* 59.

[31] Treglon, P. A.; Laurence, G. S. *J. Scient. Instrum.* **1965,** *42,* 869.

[32] Okubo, T.; Maeda Kitano, Y. *J. Phys. Chem,* **1989,** *93,* 3721.